SCIENTIFIC REPORTS

OPEN

SUBJECT AREAS:
ELECTROCHEMISTRY
SOLID-STATE CHEMISTRY
BATTERIES
GLASSES

Received
29 August 2014

Accepted
31 October 2014

Published
19 November 2014

Correspondence and requests for materials should be addressed to S.A. (afyon@inorg.chem.ethz.ch) or R.N. (reinhard.nesper@inorg.chem.ethz.ch)

New High Capacity Cathode Materials for Rechargeable Li-ion Batteries: Vanadate-Borate Glasses

Semih Afyon[1,2], Frank Krumeich[1], Christian Mensing[1], Andreas Borgschulte[3] & Reinhard Nesper[1]

[1]ETH Zurich, Department of Chemistry and Applied Biosciences, CH-8093 Zurich, Switzerland, [2]ETH Zurich, Department of Materials, CH-8093 Zurich, Switzerland, [3]Empa - Swiss Federal Laboratories for Materials Science & Technology, CH-8600 Dübendorf Switzerland.

V_2O_5 based materials are attractive cathode alternatives due to the many oxidation state switches of vanadium bringing about a high theoretical specific capacity. However, significant capacity losses are eminent for crystalline V_2O_5 phases related to the irreversible phase transformations and/or vanadium dissolution starting from the first discharge cycle. These problems can be circumvented if amorphous or glassy vanadium oxide phases are employed. Here, we demonstrate vanadate-borate glasses as high capacity cathode materials for rechargeable Li-ion batteries for the first time. The composite electrodes of V_2O_5 – $LiBO_2$ glass with reduced graphite oxide (RGO) deliver specific energies around 1000 Wh/kg and retain high specific capacities in the range of ~ 300 mAh/g for the first 100 cycles. V_2O_5 – $LiBO_2$ glasses are considered as promising cathode materials for rechargeable Li-ion batteries fabricated through rather simple and cost-efficient methods.

After the introduction of $LiFePO_4$ as a positive electrode material for LIBs, the focus of research in this field lies mainly on poly-anionic materials. However, the low theoretical capacity of $LiFePO_4$ (170 mAh/g) is a setback for its applications in batteries requiring high energy densities. This constraint is exemplified by the limited range of electric vehicles (~ < 160 km) hindering their large scale introduction. To increase energy densities, novel cathode materials beyond NMC, LFP and etc. have to be developed which utilize more than one Li per 100 atomic mass units. Owing to the many accessible oxidation states of vanadium, vanadate-based electrodes could become interesting alternatives. Consequently, there has been extensive research in order to employ on vanadates as a cathode materials that are synthesized by various methods resulting different morphologies, compositions and properties. With the use of thin film electrodes and relatively low current rates, the insertion of up to 5.8 and 4 Li per formula unit of V_2O_5 were demonstrated for aerogels[1,2] and xerogels[3–6], respectively. A single phase process was claimed for the lithiation mechanism of the xerogel-based cathodes on the observation of a steady decrease of the voltage in the discharge curve accompanied by the reduction of V^{5+} to lower oxidation states[1,7]. The high amount of lithium insertion that was stated for such thin film samples decreases to ca. 2–3 Li per V_2O_5, when standard electrodes and higher rates (~ > C/2) are used[5,8,9]. For crystalline counterparts, V_2O_5 transforms into several $Li_xV_2O_5$ phases depending on the amount of lithium inserted, α- ($x < 0.01$), ε- ($0.35 < x < 0.7$), δ- ($x = 1$), γ- ($1 < x < 2$) and ω- ($x = 3$)[10]. The phases that are formed by intercalation up to one Li per formula unit of V_2O_5 (α-, ε-, δ-$Li_xV_2O_5$) are not significantly different from the initial structure, but only a puckering of VO_5 pyramid layers occurs. These phases can be cycled in a reversible way with a theoretical capacity of ~ 147 mAh/g. In contrast, an irreversible phase transformation arises on insertion of more than 0.5 Li per V, and γ-$Li_xV_2O_5$ is formed that can be cycled without structural transformation in the range of $0 \leq x \leq 2$. This process yields a theoretical capacity of ~ 294 mAh/g. Upon deep discharge to voltages below 1.9 V, another irreversible transition occurs to ω-$Li_xV_2O_5$ with an insertion of 3 Li per formula unit[10]. With this, a large theoretical capacity of ~ 440 mAh/g is reached that is almost three times larger than that of many conventional cathode materials. ω-$Li_xV_2O_5$ cycles like a single solid solution in subsequent charge/discharge curves with an irreversible capacity loss in the first charge since all of the inserted lithium atoms cannot be extracted from the host structure (~ 0.4 Li per formula unit of $Li_3V_2O_5$ remain unexchanged)[10]. The capacity retention is a huge problem as half of the capacity vanishes within the first ten cycles for the unaltered V_2O_5 even at very low current rates (10 mA/g)[11]. Bulk V_2O_5 is also considered to be kinetically limited by its low ionic and electronic conductivities and it has been shown that the increase of current density leads to markedly reduced practical capacities[11,12].

In order to address these problems, many different approaches have been tried by various research groups. Whittingham et al. employed nanorods of V_2O_5 that were synthesized by annealing xerogels under O_2 atmosphere, and obtained a stable capacity of ca. 300 mAh/g but only for the first 10 cycles[13,14]. The enhanced performance of this material was attributed mainly to its high surface area, shorter Li diffusion lengths and facilitation of strain relaxation[13,14]. Porous monodisperse V_2O_5 microspheres were tested by Wang et al. in the voltage window of 2.05–4.0 V, and an initial discharge capacity of 276 mAh/g was realized with a fading rate of 0.38% per cycle[15]. Composite electrodes with carbon and conducting polymers were also tried. A V_2O_5/polypyrrole-composite cathode prepared by Kim et al. delivered an initial discharge capacity of ~ 425 mAh/g that decreased to ~ 250 mAh/g till the 10th cycle[16]. For a nano-V_2O_5/PEDOT composite film electrode, Song et al. reported specific capacities of ~ 262, 239, 186 and 141 mAh/g at 0.1C, 1C, 10C and 100C rates within 4.0–1.8 V, respectively[17]. Numerous other reports employing nano-particles and composite electrodes can be found in the literature[18–21].

Irreversible phase transformations and volume work leading to amorphization as well as to loss of low valence state metal ions into the electrolyte accompany most high capacity materials during cycling. To tackle these problems, we have chosen borate-based glasses of V_2O_5 in order to explore vitreous redox-active systems pursuing the goal of utilizing many oxidation states of vanadium to the highest possible extent and fixing the vanadate group by a network former to enhance cycling stability. There are a few research reports on V_2O_5 – P_2O_5 glasses as cathode materials[22–24]. Sakurai et al. reported a first discharge capacity of 500 mAh/g within 4.0–1.0 V for the V_2O_5 – P_2O_5 glass cathode[24]. The cathode material functions as a uniform material without any visible plateau, but the capacity on the first charge already drops to 350 mAh/g, and cycling properties are not very remarkable for the large potential window. For borate based binary, ternary, quaternary V_2O_5 glass systems, there had been research on vibrational, mechanical, thermal and electrical properties[25–30]. The use of V_2O_5 – B_2O_3 glass as an electrode material for secondary batteries is mentioned in a few older patents grosso modo together with other glasses[22,31] however, no electrochemical study exploring their actual utilization exists in literature, yet. Furthermore, to the best of our knowledge, V_2O_5 – $LiBO_2$ glasses (Li_2O – B_2O_3 – V_2O_5 system) and their composites have not been explored as positive electrode material yet, and here, we report on V_2O_5 – $LiBO_2$ glasses and their composites as cathode materials for rechargeable Li-ion batteries for the first time. The composite electrode of V_2O_5 – $LiBO_2$ glass with reduced graphite oxide delivers first discharge capacities around 400 mAh/g and maintain capacities in the range of ~ 300 mAh/g within the first 100 cycles. The synthesis method for the new class of electrodes is very simple and cost efficient. Comparable cathode materials delivering similar capacities and specific energies are only obtainable by laborious synthetic methods and using expensive techniques and educts.

Results & Discussion

Here, a glassy material from the Li_2O – B_2O_3 – V_2O_5 glass system, which will be referred to as V_2O_5 – $LiBO_2$ glass in the following text, is reported as a cathode material for rechargeable LIBs. A mixture of 80 wt-% V_2O_5 and 20 wt-% $LiBO_2$ is melted at 900°C. The subsequent quenching to room temperature produces the glass material. Elemental analysis performed using inductively coupled plasma optical emission spectrometry (ICP-OES) confirmed the final composition of the glass material that is in close proximity to the intended glass composition (80 wt-% V_2O_5 - 20 wt-% $LiBO_2$) (Table S1). Based on this composition, a theoretical capacity of ~ 118 mAh/g is expected for the insertion or extraction of 1 Li per formula unit of V_2O_5 – $LiBO_2$ glass.

The XRD powder pattern of the V_2O_5 – $LiBO_2$ glass material is shown in Fig. 1a. In the XRD pattern, the glassy product exhibits a high background lacking any Bragg reflections. The differential thermal analysis (DTA) proves the glassy nature of the quenched 80-20 wt-% V_2O_5 – $LiBO_2$ material (Fig. S1). The endothermic effect at ~ 205°C arises from the glass transition, followed by transformations into crystalline phases around 218°C and 325°C that are indicated by exothermic peaks. The melting region for the crystalline phases corresponds to a range of ~ 550–650°C, as it can be estimated from the heating curve.

Fig. 1b depicts infrared (IR) spectra of the V_2O_5 – $LiBO_2$ glass and the educts, V_2O_5 (99.2%, Alfa Aesar) and $LiBO_2$ (99.9%, Alfa Aesar). The IR spectrum of the V_2O_5 – $LiBO_2$ glass is very different from the spectra of the educts proving the formation of a new kind of material. The strong band observed for V_2O_5 at ca. 1020 cm^{-1} stemming from the stretching mode of the vanadyl group V = O in the VO_5 square pyramids disappears in the spectrum of the V_2O_5 – $LiBO_2$ glass probably indicating the loss of localized double bond. A weak band emerging at ~ 970–980 cm^{-1} could still be attributed to the stretching of V = O with a decrease in bond order, but this band together with the ones at ~ 890–900 cm^{-1} and ~ 1090–1100 cm^{-1} could also be assigned to the asymmetric stretching vibrations of BO_4 tetrahedral units that are expected to appear between 850 and 1100 cm^{-1} [32–35]. This finding also fits well with the influence of alkali metal oxide addition into borate glass: The addition of an alkali metal oxide (e.g. Li_2O) to borate glasses was discussed to alter the glass network by the conversion of trigonal BO_3 groups from the boroxol rings to BO_4 groups; thus, increasing the number of structural linkages through B – O – B bonds[36,37]. Though some BO_3 groups are converted to tetrahedral units, they are still present in the glass network as the bands observed between 1200 and 1600 cm^{-1} are related to the asymmetric stretching modes of BO_3 trigonal units[32,33].

Scanning electron microscopy (SEM) images of the V_2O_5 – $LiBO_2$ glass are displayed in Fig. 2. When the glass forming melt is quenched, a homogeneous disk of glass is obtained. Fig. 2a depicts a side image of V_2O_5 – $LiBO_2$ glass disk with a thickness of ~ 200 microns. The homogenous nature can also be observed under an optical microscope with a gleaming purple appearance similar to volcanic glass. These large glass pieces have to be grinded in order to make further characterizations and to form electrodes of the material. The particles can be crushed down to a spread between micron and sub-micron size (Fig. 2b) in an agate mortar by extensive grinding. Yet, some large pieces of 40–50 microns in size are still present (Fig. 2b).

Micron-sized blocks of the glass material can be seen in transmission electron microscopy images (TEM) (Fig. 2c). As revealed by bulk characterization techniques, the state is mostly amorphous being further verified here with a lack of order even at 5–10 nm resolution for many parts of the sample (Fig. 2d). Electron diffraction patterns lacking any reflections further support the glassy nature of the material (Fig. S2). However, lattice fringes with a spacing of about 9.5 Å extending into nano-crystallites with sizes in the range of 20–30 nm are also found in some regions (Fig. S3). The d-distance (~ 9.5 Å) corresponds to 2Θ = ~ 9.3, where a broad reflection from $Li_xV_2O_5$ phases ($Li_{0.3}V_2O_5$ (ICSD 166482)) appears, in the XRD powder pattern of the V_2O_5 – $LiBO_2$ glass, if heated above the glass transition temperature (Fig. S4). Thus, it can be concluded that seldom occurring nano-crystallites of $Li_xV_2O_5$ are embedded in the amorphous glass matrix.

For a typical fabrication of the V_2O_5 – $LiBO_2$ glass electrode, (70 wt-%) active material, (20 wt-%) conductive carbon (Super P® Timcal) and (10 wt-%) PVDF binders were manually mixed in an agate mortar without any ball-milling. The cells built from such electrodes were tested in a galvanostatic mode by first discharging to 1.5 V and then charging to 4.0 V at a rate of 50 mA/g. The reported specific capacities here are based on the active mass of

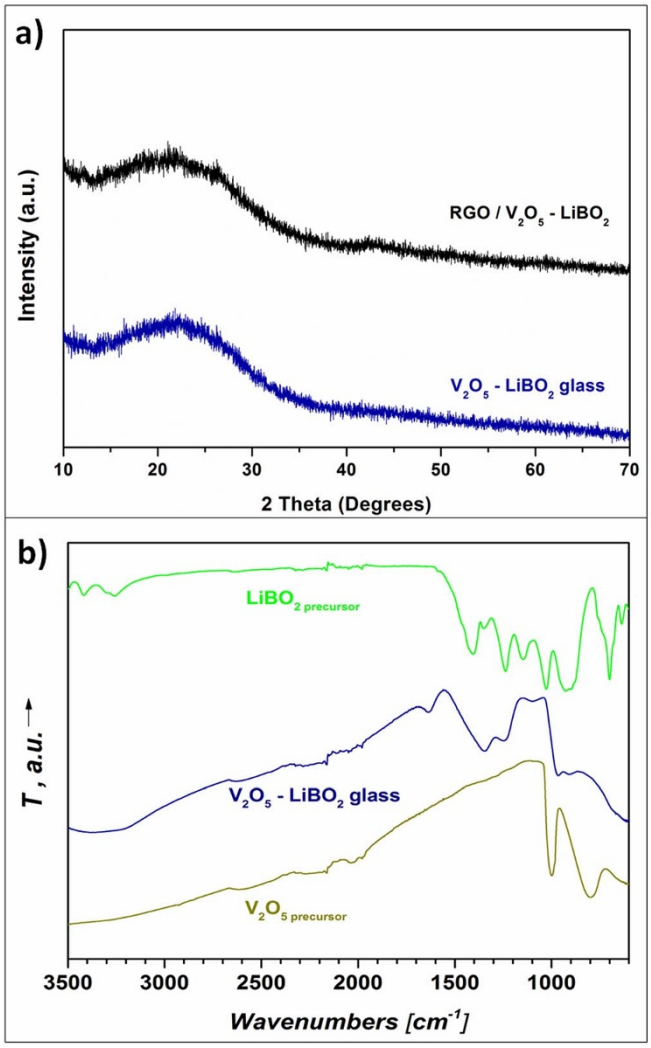

Figure 1 | (a) XRD powder patterns of V_2O_5 – $LiBO_2$ glass and RGO/V_2O_5 – $LiBO_2$ glass composite, (b) Infrared (IR) spectra of the V_2O_5 – $LiBO_2$ glass, and V_2O_5 and $LiBO_2$ precursors.

V_2O_5 – $LiBO_2$ glass; not exclusively on the mass of V_2O_5. The first ten galvanostatic charge/discharge curves of the V_2O_5 – $LiBO_2$ glass are displayed in Fig. 3a. The voltage declines continuously with increasing lithium insertion into the material and featureless curves without a multi-step behavior appear that is consistent with the expected homogeneous phase lithiation mechanism of a glass material. A first discharge capacity of 327 mAh/g is obtained, and the cell is charged with a capacity of 308 mAh/g in the subsequent cycle. This finding shows that the huge capacity loss associated with irreversible phase transformation of crystalline V_2O_5 materials is largely circumvented for the V_2O_5 – $LiBO_2$ glass investigated here. Fig. 3b shows the rate capability for the V_2O_5 – $LiBO_2$ glass within 1.5–4.0 V. The capacities in the range of ~ 293, 236 and 180 mAh/g are delivered at rates of 50, 100 and 200 mA/g, respectively. The discharge capacity drastically drops to 125 mAh/g at the 35th cycle, when the rate is increased to 400 mA/g, and recovers to 260 mAh/g at the 45th cycle when the rate is 50 mA/g. Limited capacities at high rates are probably caused by poor kinetics of the glassy material, especially for the larger particles of the V_2O_5 – $LiBO_2$ glass that were found to range from 2 to 50 microns in diameter (Fig. 2b).

In order to tackle this problem and further improve cycling properties with higher charge/discharge capacities, a composite electrode of the V_2O_5 – $LiBO_2$ glass with reduced graphite oxide (RGO) was employed. The preparation of the composite electrode includes steps of ball-milling the active material with graphite oxide (GO) and reducing GO afterwards at ~ 200°C. No major diffraction peaks of graphite oxide are detected in the powder pattern of the composite material indicating the delamination and partial reduction of graphite oxide (Fig. 1a). However, in line with the results of differential thermal analysis (DTA), heating above the glass transition temperature (~ 205°C) leads to the crystalline phases, and consequently, a glass ceramic composite (Fig. S4 & S5).

Scanning electron microscopy (SEM) images of the RGO/V_2O_5 – $LiBO_2$ glass composite show that the large glass pieces were ground to sub-micron sizes and a fine mixture with reduced graphite oxide was achieved (Fig. S6). However, some large flakes of reduced graphite oxide in a wrinkled morphology can also be found at some regions of the composite (Fig. S6). The large flakes of RGO may still be useful in terms of providing better long range conduction in the electrode composite. Transmission electron microscopy images (TEM) reveal more information on covering and interaction of the V_2O_5 – $LiBO_2$ glass with reduced graphite oxide (RGO). Some parts of the glass material are directly coated by only a few layers of RGO as shown in Fig. 2e & Fig. S5. Widespread coating provided by the flocculated RGO is also observed (Fig. S7). The interlayer distance found for the flocculated RGO, ~ 4.3 Å, and also, the XPS characterization of the RGO/V_2O_5 – $LiBO_2$ glass composite provide further evidence for the partial reduction of graphite oxide and the formation of RGO on glass particle surfaces (Fig. S8 & S10). Both the direct RGO coating of the glass surfaces and clustering of RGO between the V_2O_5 – $LiBO_2$ glass particles, respectively, are expected to improve short and long range conductivity within the composite electrode.

The cells with a cathode composition of ~ 74 wt-% active material, ~ 16 wt-% conductive carbon originating from the RGO (no additional carbon black) and ~ 10 wt-% PVDF were cycled between 1.5 V and 4.0 V at a rate of 50 mA/g. Similar to the plain glass material, the reported specific capacities for the composite electrode material are calculated based on the active mass of V_2O_5 – $LiBO_2$ glass; not exclusively on the mass of V_2O_5, and RGO is considered as an inactive part in the potential window of our interest, as well. The first ten galvanostatic charge/discharge curves of the RGO/V_2O_5 – $LiBO_2$ glass composite are shown in Fig. 4a. The first discharge capacity has been raised to ~ 405 mAh/g for the composite electrode. This capacity corresponds to the insertion of ~ 3.4 Li per formula unit of V_2O_5 – $LiBO_2$ glass. A high capacity of ~ 390 mAh/g is reached in the subsequent charge proving that the RGO/V_2O_5 – $LiBO_2$ glass composite also does not suffer from the large irreversible capacity loss associated with the phase transformations of crystalline V_2O_5. Remarkably, this initial charge capacity is largely preserved in the range of ~ 300 mAh/g within the first 100 cycles (Fig. 4c). If the cell is charged to 4.5 V first, the glass material can be also delithiated resulting a first charge capacity of ~ 20–25 mAh/g, however, the cycling stability is found to be rather poor in the large potential window (Figure S12 & S13). The electrochemical activity in the first charge also indicates the presence of the partially reduction of V^{5+} species to V^{4+} species in the glass material. Based on the obtained first charge capacity, the formation of $Li_{0.3}V_2O_5$ phases above the glass transition, XPS and magnetic measurements (Fig. S9, S10 and S11), the averaged oxidation state for vanadium in the glassy electrode materials can be given as ~ 4.8–4.9 +. The sloping characteristic of the galvanostatic charge/discharge curves again indicates a homogeneous phase process. The rate capability for the RGO/V_2O_5 – $LiBO_2$ glass composite has been enhanced as well. Fig. 4b shows the rate capability within first 50 galvanostatic cycles between 1.5 V and 4.0 V. For rates of 50, 100, 200 and 400 mA/g, average discharge capacities are ~ 388, 355, 329 and 299 mAh/g, respectively. When the rate is changed back from 400 mA/g to 50 mA/g, the discharge capacity recovers from 298 mAh/g to ~ 370 mAh/g at the 42nd cycle. The specific energy is ~ 900 $Whkg^{-1}$ with an average discharge voltage of ~ 2.4 V at this

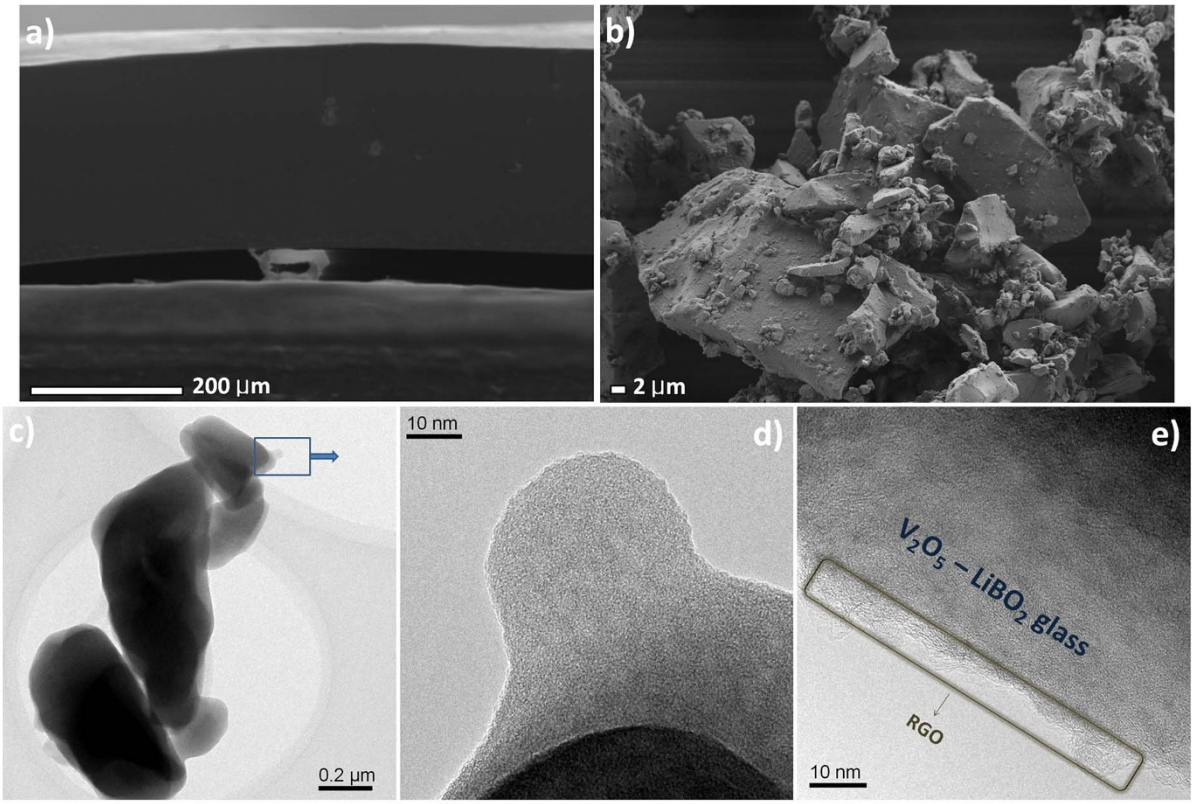

Figure 2 | Scanning electron microscopy (SEM) images of the V_2O_5 – $LiBO_2$ glass displaying (a) a side view of glass disk, (b) an overview of a ground sample showing micron – sub-micron sized glass particles; Transmission electron microscopy images (TEM) displaying (c) an agglomerate of V_2O_5 – $LiBO_2$ glass particles, (d) the amorphous nature of the V_2O_5 – $LiBO_2$ glass, (e) the RGO/V_2O_5 – $LiBO_2$ glass composite with a fine coating of reduced graphite oxide (RGO).

cycle. The favorable response of the electrochemical system to higher charge/discharge rates demonstrates the improvements arising from the composite electrode. The capacity delivered at the highest rate (400 mA/g) is more than doubled compared to the amount obtained for the V_2O_5 – $LiBO_2$ glass electrode without RGO. The improvement made with ball-milling and conductive coating is encouraging as it shows that the problem is mainly stemming from the kinetic problems associated with the larger glass particles. Clearly, further optimization of the electrochemical performance can be expected by improving the composite characteristics.

Discussion

The galvanostatic cycling analysis of vanadate – borate glasses shows featureless curves without any distinct voltage plateau starting from the first discharge; this supports the understanding of a glassy electrode material. Similar to the other V_2O_5 based amorphous cathode materials[1–6], more than 3 Li per formula unit can be inserted to vanadate-borate glass electrodes. The amorphous nature of the glass electrodes is also largely preserved upon lithium insertion and extraction (Fig. S14); however, further investigations that are beyond the scope of this current work could be performed to deeply understand the lithiation/delithiation processes. Nevertheless, the notable electrochemical properties for vanadate – borate glasses are mainly attributed to the absence of a long range order that allows for subtle structural adaptations, which cannot occur within crystalline phases. This is markedly different from the huge capacity loss observed for crystalline V_2O_5 phases in the first cycle related to the irreversible phase transformation to ω-$Li_3V_2O_5$, which cannot be cycled to its full extent within 1.5–4.0 V. Besides, crystalline phases tend to deteriorate during large redox work showing itself as capacity fading under extensive cycling[13–15,38–40]. The borate glass former constitutes a kind of glue to low valence vanadium species, too. Thus, well-known problems of crystalline V_2O_5 electrodes can be circumvented in a glassy vanadium oxide electrode. Furthermore, the RGO/V_2O_5 – $LiBO_2$ glass composite provides a much enhanced electrochemical performance. This can be traced back to a number of reasons: 1. In comparison to the other composite electrodes with reduced graphite oxide[41–43], there are common features arising from the RGO network that is expected to facilitate Li^+ ion as well as electron transports, prevent contact losses under extensive cycling and may act as a protective layer against cycling by-products. 2. In addition to common characteristics with previously demonstrated systems, a much finer coating of particles is found for the V_2O_5 – $LiBO_2$ glass with only a few layers of RGO. 3. The direct coating of the surface and the network formation via reduced graphite oxide seemingly improves short and long range conductivity, respectively. 4. Effects of particle size are also very prominent for the V_2O_5 – $LiBO_2$ glass system, as noticeably better kinetic properties are attained for smaller particles in terms of a decreased polarization and a better rate capability.

In conclusion, vanadate-borate glasses have been demonstrated as inexpensive, high capacity cathode materials for the first time. The RGO/V_2O_5 – $LiBO_2$ composite electrode delivers first discharge capacities around 400 mAh/g and maintains high capacities in the range of ~ 300 mAh/g for the first 100 cycles (between 1.5 V and 4.0 V at 50 mA/g rate)! The rate capability of the composite electrode is also notable with a discharge capacity of ~ 299 mAh/g (35^{th} cycle) at 400 mA/g rate. Clearly, higher charge/discharge capacities and enhanced cycling stabilities compared to bulk and various nano-forms of V_2O_5 have been demonstrated here for vanadate – borate glasses. For practical battery applications, the overall cycling stability may still be improved via better cell and electrode engineering,

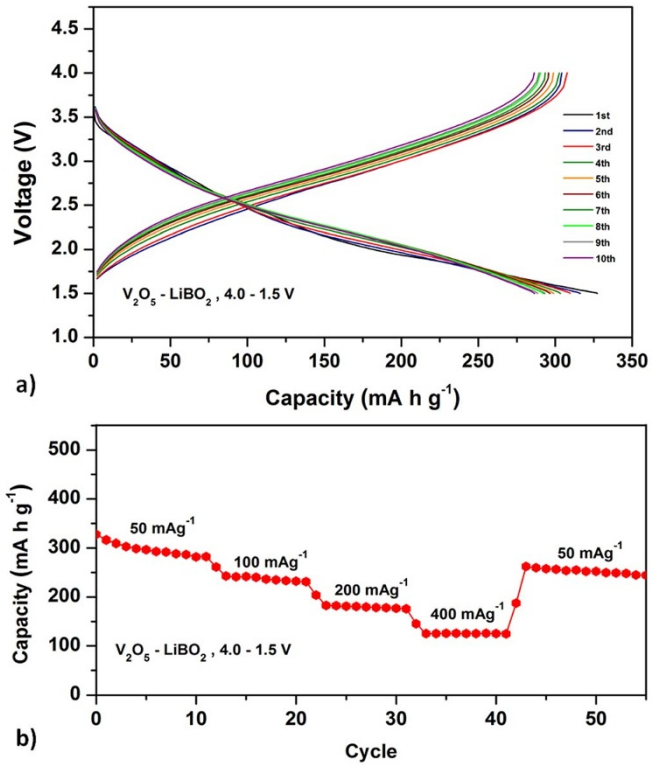

Figure 3 | (a) The first ten charge/discharge curves of the V_2O_5 – $LiBO_2$ glass within a potential window of 1.5 – 4.0 V at 50 mA/g rate, (b) the rate capability of the V_2O_5 – $LiBO_2$ glass within 1.5–4.0 V at 50, 100, 200 and 400 mA/g rates (at room temperature).

the exploration of different protective coatings and more stable electrolyte systems. Nevertheless, the results obtained for vanadate – borate glasses are very encouraging and may trigger further studies for similar glass systems that could encompass the practical use of glassy materials as next generation electrode materials for rechargeable Li-ion batteries.

Methods

Synthesis of V_2O_5 – $LiBO_2$ glass and reduced graphite oxide (RGO) composite. V_2O_5 – $LiBO_2$ glass was obtained with a glass forming procedure. V_2O_5 (99.2%, Alfa Aesar) and $LiBO_2$ (99.9% Alfa Aesar) analytical pure grade powders in corresponding amounts (e.g. 4 g V_2O_5 and 1 g $LiBO_2$ for 80 : 20 wt-% V_2O_5 : $LiBO_2$ glass) were thoroughly mixed and ground in an agate mortar, and thereafter, the mixtures were placed in Pt crucibles. The crucibles were heated in a muffle furnace at 900°C, and homogeneous melts were obtained after 30–60 min. of heat treatment. Then, melts were quenched between Cu plates yielding V_2O_5 – $LiBO_2$ glass. The produced glass disks were pulverized in an agate mortar for further characterizations. The composite with reduced graphite oxide was prepared by ball-milling ~ 66.6 wt-% active material with ~ 33.3 wt-% graphite oxide that was followed by the heat treatment for the reduction (9 hours under Ar atmosphere at 200°C). The final carbon content of the composite material was found to be ~ 18 wt-% by combustion-infrared spectroscopy analysis (LECO instruments, ETH LOC Micro-Laboratory).

Characterization. Powder X-ray diffraction patterns of the samples were acquired with a STOE Stadi P diffractometer equipped with a germanium monochromator and $CuK_{\alpha 1}$ radiation (40 kV, 35 mA). Differential thermal analysis (DTA) was performed with a NETZSCH STA 409 C/CD. Samples were planted in Pt crucibles, and heating/cooling curves between room temperature and 930°C were obtained under air flow. FT-IR spectra were recorded with a Thermo Scientific Nicolet iS10 Smart iTR. Scanning electron microscopy (SEM) analysis of samples were carried out with a Zeiss Gemini 1530 operated at 1 kV. Transmission electron microscopy (TEM) analysis was performed with a Tecnai F30 microscope (FEI; field emission gun), operated at 300 kV, point resolution of ~ 2Å. Solution nebulization inductively coupled plasma optical emission spectrometry (SN-ICPOES) was carried out using an Arcos instrument (Spectro Analytical Instruments, Germany). The digestions of glass materials for ICP-OES analysis were done in concentrated HNO_3 with an Ultraclave II microwave digestion (200°C at 40 bars, 30 min) unit, and the solutions were treated with H_2O_2 afterwards. Magnetic measurements were carried out with a SQUID magnetometer (MPMS 5S, Quantum Design) between 300 and 2 K under constant

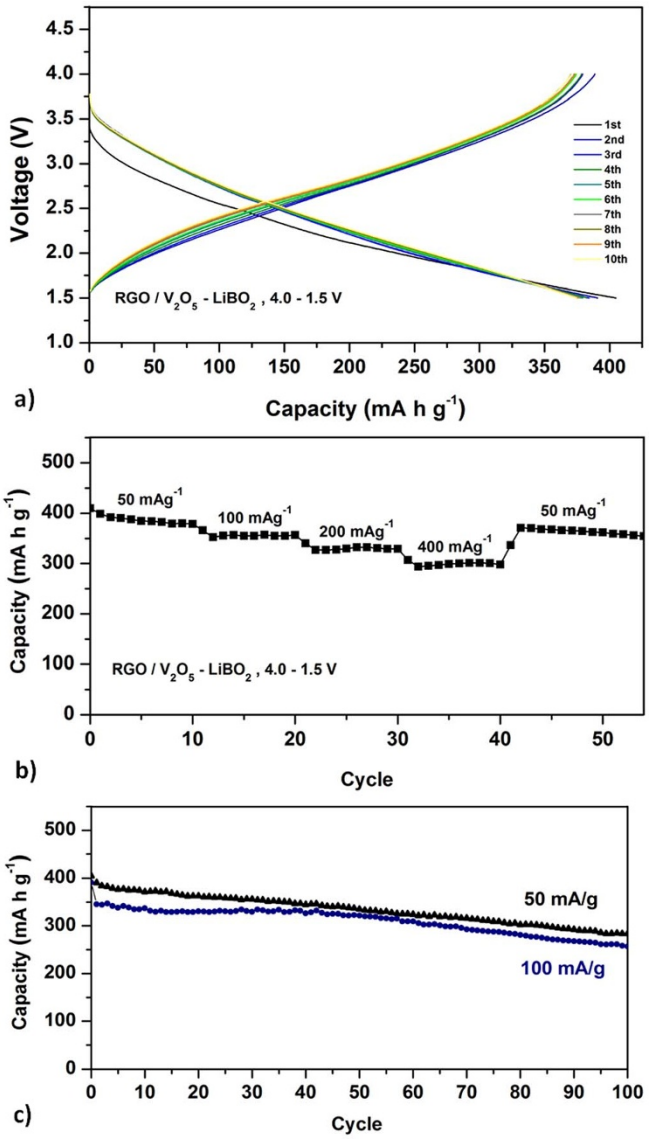

Figure 4 | (a) The first ten charge/discharge curves of the RGO/V_2O_5 – $LiBO_2$ glass composite in a potential window of 1.5–4.0 V at 50 mA/g rate, (b) the rate capability of the RGO/V_2O_5 – $LiBO_2$ glass composite within 1.5–4.0 V at 50, 100, 200 and 400 mA/g rates (at room temperature), (c) discharge capacity vs. cycle number for the RGO/V_2O_5 – $LiBO_2$ glass composite within 1.5–4.0 V at 50 and 100 mA/g rates.

field strength. XPS surface analysis was performed in a modified VG EscaLab spectrometer with a base pressure below 10^{-9} mbar. The sample powder was spread onto a carbon tape inside an Ar glove box (impurity levels below $O_2 < 1$ ppm and $H_2O < 1$ ppm) directly connected to the spectrometer and transferred without exposure to ambient conditions. XPS spectra were collected with a SPECS PHOIBOS 100 analyzer using a non-monochromatic X-ray source (Al K alpha: 1486 eV). Due to the charge shift, the binding energy was re-calibrated using the O1s peak set to 530.0 eV.

Electrochemical tests. For electrode fabrication of composite materials with RGO, no additional carbon black was used, and (90 wt-%) composite powder was thoroughly mixed with (10 wt-%) PVDF binder in an agate mortar. The mixture was ultrasonically dispersed in 1 : 4 toluene : THF solution. The resulting slurry was cast on Ti current collectors and dried at 80°C under vacuum. The dried electrodes had approximately 5 mg electrochemically active material (a loading of ~ 4–5 mg/cm²). The plain electrodes without any carbon resulting from the composite were constructed in the same way, but the initial powder mixture was prepared with (70 wt-%) active material, (20 wt-%) conductive carbon (Super P® Li Timcal) and (10 wt-%) PVDF binder. Li metal anodes were prepared from a 0.75 mm-thick ribbon (Aldrich), and 1 M solution of $LiPF_6$ in EC : DMC (1 : 1) (Merck, LP-30 SelectiLyte™) served as the electrolyte. Swagelok type cells were built in an Ar filled glove-box. Galvanostatic measurements were performed in the voltage range of 1.5–4.0 V at a

usual rate of 50 mA/g. Rate capability tests were done with ~ 10 cycle blocks at varying rates 50, 100, 200, 400 mA/g, and then again 50 mA/g; the rates were successively altered after a charging section. The reported specific capacities were calculated based on the active mass of V_2O_5 – $LiBO_2$ glass; not exclusively on the mass of V_2O_5.

1. Le, D. B. *et al*. High surface area V2O5 aerogel intercalation electrodes. *J Electrochem Soc* **143**, 2099–2104, doi:Doi 10.1149/1.1836965 (1996).
2. Passerini, S. *et al*. XAS and electrochemical characterization of lithiated high surface area V2O5 aerogels. *Solid State Ionics* **104**, 195–204, doi:Doi 10.1016/S0167-2738(97)00438-4 (1997).
3. Le, D. B., Passerini, S., Tipton, A. L., Owens, B. B. & Smyrl, W. H. Aerogels and Xerogels of V2o5 as Intercalation Hosts. *J Electrochem Soc* **142**, L102–L103, doi:Doi 10.1149/1.2044250 (1995).
4. Passerini, S., Chang, D., Chu, X., Le, D. B. & Smyrl, W. Spin-Coated V2o5 Xerogel Thin-Films .1. Microstructure and Morphology. *Chem Mater* **7**, 780–785, doi:Doi 10.1021/Cm00052a025 (1995).
5. Lira-Cantu, M. & Gomez-Romero, P. The hybrid polyaniline/V2O5 xerogel and its performance as cathode in rechargeable lithium batteries. *J New Mat Electr Sys* **2**, 141–144 (1999).
6. Livage, J. Vanadium Pentoxide Gels. *Chem Mater* **3**, 578–593, doi:Doi 10.1021/Cm00016a006 (1991).
7. Passerini, S. *et al*. XAS and electrochemical characterization of lithium intercalated V2O5 xerogels. *Solid State Ionics* **90**, 5–14, doi:Doi 10.1016/S0167-2738(96)00380-3 (1996).
8. Owens, B. B., Passerini, S. & Smyrl, W. H. Lithium ion insertion in porous metal oxides. *Electrochim Acta* **45**, 215–224, doi:Doi 10.1016/S0013-4686(99)00205-4 (1999).
9. Tipton, A. L., Passerini, S., Owens, B. B. & Smyrl, W. H. Performance of lithium/V2O5 xerogel coin cells. *J Electrochem Soc* **143**, 3473–3477, doi:Doi 10.1149/1.1837239 (1996).
10. Delmas, C., Cognacauradou, H., Cocciantelli, J. M., Menetrier, M. & Doumerc, J. P. The Lixv2o5 System - an Overview of the Structure Modifications Induced by the Lithium Intercalation. *Solid State Ionics* **69**, 257–264, doi:Doi 10.1016/0167-2738(94)90414-6 (1994).
11. Glushenkov, A. M. *et al*. A novel approach for real mass transformation from V2O5 particles to nanorods. *Cryst Growth Des* **8**, 3661–3665, doi:Doi 10.1021/Cg800257d (2008).
12. Leger, C., Bach, S., Soudan, P. & Pereira-Ramos, J. P. Structural and electrochemical properties of omega-Li(x)V(2)O(5) (0.4 <= x <= 3) as rechargeable cathodic material for lithium batteries. *J Electrochem Soc* **152**, A236–A241, doi:Doi 10.1149/1.1836155 (2005).
13. Ban, C. M., Chernova, N. A. & Whittingham, M. S. Electrospun nano-vanadium pentoxide cathode. *Electrochem Commun* **11**, 522–525, doi:DOI 10.1016/j.elecom.2008.11.051 (2009).
14. Lutta, S. T., Dong, H., Zavalij, P. Y. & Whittingham, M. S. Synthesis of vanadium oxide nanofibers and tubes using polylactide fibers as template. *Mater Res Bull* **40**, 383–393, doi:DOI 10.1016/j.materresbull.2004.10.005 (2005).
15. Wang, S. Q. *et al*. Porous monodisperse V2O5 microspheres as cathode materials for lithium-ion batteries. *J Mater Chem* **21**, 6365–6369, doi:Doi 10.1039/C0jm04398b (2011).
16. Kim, Y. *et al*. Increase in Discharge Capacity of Li Battery Assembled with Electrochemically Prepared V2O5/polypyrrole-composite-film Cathode. *B Kor Chem Soc* **31**, 3109–3114, doi:DOI 10.5012/bkcs.2010.31.11.3109 (2010).
17. Song, H. M. *et al*. Electrochemical Impedance Analysis of V2O5 and PEDOT Composite Film Cathodes. *Electroanal* **23**, 2094–2102, doi:DOI 10.1002/elan.201100177 (2011).
18. Yin, H. H. *et al*. Porous V2O5 micro/nano-tubes: Synthesis via a CVD route, single-tube-based humidity sensor and improved Li-ion storage properties. *J Mater Chem* **22**, 5013–5019, doi:Doi 10.1039/C2jm15494c (2012).
19. Liu, Y. Y. *et al*. V2O5 Nano-Electrodes with High Power and Energy Densities for Thin Film Li-Ion Batteries. *Adv Energy Mater* **1**, 194–202, doi:DOI 10.1002/aenm.201000037 (2011).
20. Inamoto, M., Kurihara, H. & Yajima, T. Electrode Performance of Vanadium Pentoxide Xerogel Prepared by Microwave Irradiation as an Active Cathode Material for Rechargeable Magnesium Batteries. *Electrochemistry* **80**, 421–422, doi:DOI 10.5796/electrochemistry.80.421 (2012).
21. Huguenin, F., Malta, M., Torresi, R. & Buttry, D. A. Electrochemical and electrogravimetric behavior of composite formed by polyaniline and vanadium pentoxide. *Elec Soc S* **215**, 220–229 (2003).
22. Sakurai, Y., Hirai, T., Okada, S., Okada, T., Yamaki, J. & Ohtsuka, H. inventors; Nippon Telegraph And Telephone Corporation, assignee. Lithium Battery Including Vanadium Pentoxide Based Amorphous Cathode Active Material. United States Patent US 4675260 A. 1987 Jun 23.
23. Sakurai, Y. & Yamaki, J. V2o5-P2o5 Glasses as Cathode for Lithium Secondary Battery. *J Electrochem Soc* **132**, 512–513, doi:Doi 10.1149/1.2113874 (1985).
24. Sakurai, Y. & Yamaki, J. Correlation between Microstructure and Electrochemical-Behavior of Amorphous V2o5-P2o5 in Lithium Cells. *J Electrochem Soc* **135**, 791–796, doi:Doi 10.1149/1.2095773 (1988).
25. Kundu, V., Dhiman, R. L., Goyal, D. R. & Maan, A. S. Physical and electrical properties of semiconducting Fe2O3-V2O5-B2O3 glasses. *Optoelectron Adv Mat* **2**, 428–432 (2008).
26. Padmasree, K. P. & Kanchan, D. K. Modulus studies of CdI2-Ag2O-V2O5-B2O3 system. *Mat Sci Eng B-Solid* **122**, 24–28, doi:DOI 10.1016/j.mseb.2005.04.011 (2005).
27. Khasa, S., Seth, V. P., Gupta, S. K. & Krishna, R. M. EPR and DSC study of M2O.V2O5.B2O3 (M= Li, Na or K) glasses. *Phys Chem Glasses* **40**, 269–272 (1999).
28. Kashif, I., Sanad, A. M. & Abozeid, Y. M. Study of Some Physical-Properties of the V2o5-B2o3-P2o5-Fe2o3 Glass System. *Phys Chem Glasses* **31**, 196–198 (1990).
29. Culea, E. & Nicula, A. Electrical-Properties of V2o5-B2o3 Glasses. *Solid State Commun* **58**, 545–549, doi:Doi 10.1016/0038-1098(86)90793-3 (1986).
30. Sharma, B. K., Dube, D. C. & Mansingh, A. Preparation and Characterization of V2o5-B2o3 Glasses. *J Non-Cryst Solids* **65**, 39–51, doi:Doi 10.1016/0022-3093(84)90353-3 (1984).
31. Tobishima, S.-i., Arakawa, M., Hirai, T. & Yamaki, J. inventors; Nippon Telegraph And Telephone Corporation, assignee. Secondary Lithium Battery. United States Patent US 4737424 A. 1988 Apr 12.
32. Khattak, G. D. & Mekki, A. Structure and electrical properties of SrO-borovanadate (V2O5)(0.5)(SrO)(0.5-y)(B2O3)(y) glassses. *J Phys Chem Solids* **70**, 1330–1336, doi:DOI 10.1016/j.jpcs.2009.06.023 (2009).
33. Hogarth, C. A. & Ahmed, M. M. Infrared-Absorption Spectroscopy of Zinc Borate and Vanadium Borate Glasses. *J Mater Sci Lett* **2**, 649–652, doi:Doi 10.1007/Bf00720388 (1983).
34. Iordanova, R., Dimitriev, Y., Kashchieva, E. & Klissurski, D. Glasses in the B2O3-V2O5 system obtained by fast quenching. *Ceram-Silikaty* **45**, 115–118 (2001).
35. Moustafa, Y. M., Hassan, A. K., ElDamrawi, G. & Yevtushenko, N. G. Structural properties of V2O5-Li2O-B2O3 glasses doped with copper oxide. *J Non-Cryst Solids* **194**, 34–40, doi:Doi 10.1016/0022-3093(95)00465-3 (1996).
36. Shkrob, I. A., Tadjikov, B. M. & Trifunac, A. D. Magnetic resonance studies on radiation-induced point defects in mixed oxide glasses. I. Spin centers in B2O3 and alkali borate glasses. *J Non-Cryst Solids* **262**, 6–34, doi:Doi 10.1016/S0022-3093(99)00668-7 (2000).
37. Shkrob, I. A., Tadjikov, B. M. & Trifunac, A. D. Magnetic resonance studies on radiation-induced point defects in mixed oxide glasses. II. Spin centers in alkali silicate glasses. *J Non-Cryst Solids* **262**, 35–65, doi:Doi 10.1016/S0022-3093(99)00669-9 (2000).
38. Oh, S.-M. *et al*. High-Performance Carbon-LiMnPO4 Nanocomposite Cathode for Lithium Batteries. *Advanced Functional Materials* **20**, 3260–3265, doi:10.1002/adfm.201000469 (2010).
39. Afyon, S., Worle, M. & Nesper, R. A Lithium-Rich Compound Li7Mn(BO3)(3) Containing Mn2+ in Tetrahedral Coordination: A Cathode Candidate for Lithium-Ion Batteries. *Angew Chem Int Edit* **52**, 12541–12544, doi:DOI 10.1002/anie.201307655 (2013).
40. Yabuuchi, N., Makimura, Y. & Ohzuku, T. Solid-state chemistry and electrochemistry of LiCo1/3Ni1/3Mn1/3O2 for advanced lithium-ion batteries III. Rechargeable capacity and cycleability. *J Electrochem Soc* **154**, A314–A321, doi:Doi 10.1149/1.2455585 (2007).
41. Zhu, K. *et al*. Synthesis of H2V3O8/Reduced Graphene Oxide Composite as a Promising Cathode Material for Lithium-Ion Batteries. *Chempluschem* **79**, 447–453 doi:10.1002/cplu.201300331 (2014).
42. Chang, J. *et al*. Multilayered Si Nanoparticle/Reduced Graphene Oxide Hybrid as a High-Performance Lithium-Ion Battery Anode. *Adv Mater* **26**, 758–764 doi:10.1002/adma.201302757 (2013).
43. Afyon, S., Kundu, D., Krumeich, F. & Nesper, R. Nano LiMnBO3, a high-capacity cathode material for Li-ion batteries. *J Power Sources* **224**, 145–151, doi:10.1016/j.jpowsour.2012.09.099 (2013).

Acknowledgments

Authors thank ETH Zurich-Trace Element and Micro Analysis Group for the solution nebulization inductively coupled plasma optical emission spectrometry (SN-ICPOES)-elemental analysis. The electron microscopy work was performed at ScopeM (Scientific Center for Optical and Electron Microscopy, ETH Zurich).

Author contributions

S.A. and R.N. planned the research project; S.A. conducted the experiments. F.K. did electron microscopy analysis. C.M. did magnetic measurements. A.B. performed XPS analysis-characterization. S.A. wrote the main manuscript text and prepared figures, and all authors reviewed the manuscript.

Additional information

Supplementary information accompanies this paper at http://www.nature.com/scientificreports

Competing financial interests: The authors declare no competing financial interests.

How to cite this article: Afyon, S., Krumeich, F., Mensing, C., Borgschulte, A. & Nesper, R. New High Capacity Cathode Materials for Rechargeable Li-ion Batteries: Vanadate-Borate Glasses. *Sci. Rep.* **4**, 7113; DOI:10.1038/srep07113 (2014).